# Study on charge transport in amorphous TCTA: an improved mobility model and its numerical simulation

L. H. LUO*, L. G. WANG, H. L. XIAO, L. M. ZHAO
*College of Electronic & Information Engineering , Guangdong Ocean University, Zhanjiang, 524088, People's Republic of China*

An accurate model for the carrier mobility of amorphous organic semiconductors is crucial for describing the characteristics of electronic devices. Although the original extended Gaussian disorder model (EGDM) effectively describes the dependence of mobility on temperature and carrier concentration, and simplifies the lattice structure, certain limiting conditions do not align with established assumptions, leading to errors. Therefore, this paper develops an improved model that not only addresses the aforementioned limitations but also calculates the carrier mobility within the simulation framework by solving the master equation. A universal and concise formula is derived to describe the charge mobility through the Marcus hopping mechanism in a disordered energy environment composed of Gaussian density of states (DOS), with parameters determined by precise numerical results. Research on the small-molecule organic semiconductor TCTA shows that experimental data are highly consistent with the results fitted by the improved model. Furthermore, the enhanced mobility model uses a calibrated effective temperature instead of the actual temperature, increasing its dependence on the electric field, and thereby more accurately reflecting the hopping transport laws of disordered organic semiconductors through random spatial positions. Finally, using this improved method, the distribution characteristics of charge carrier density and electric field in TCTA within polymer layers are analyzed in detail.

(Received July 26, 2024; accepted December 4, 2025)

*Keywords*: Molecular semiconductors, Improved model, Electric field, Effective temperature

## 1. Introduction

In the pursuit of breakthroughs in the field of low-cost photonics, especially in the development of efficient organic light-emitting diodes (OLEDs), organic photovoltaic (OPV) devices, and high mobility field-effect transistors, it is crucial to deeply understand and master the electronic characteristics of amorphous molecular semiconductors [1-7]. In these materials, charge transport is accomplished through incoherent hopping between molecular sites with random energies. These lightweight, transparent, solution-processable, and cost-effective materials rely heavily on their carrier mobility ( $\mu$ ) for their main performance metrics. It is the need for an in-depth understanding and description of carrier mobility that has spurred the proposal and development of various theoretical models. In the Gaussian disorder model (GDM) proposed by Bässler et al. [8], they assumed no spatial correlation between the energies of molecular sites and adopted a Gaussian energy spectrum of localized state distribution to describe the hopping conduction characteristics within semiconductors. However, considering the role of dipole moments in organic semiconductors, the positional energy is actually correlated with spatial location. This led to the development of the correlated disorder model (CDM) [9,10], which can describe the dependence of carrier mobility on external electric fields. Further research shows that the mobility based on the hopping mechanism depends strongly not only on temperature ( $T$ ) and electric field ( $F$ ) but also on carrier concentration ( $p$ ). Therefore, building on the Gaussian disorder model (GDM) and the correlated disorder model (CDM), researchers have further developed extended versions of these two models, known as the extended Gaussian disorder model (EGDM) and the extended correlated disorder model (ECDM) [11,12], by simulating mobilities at different carrier concentrations. The evolution of these models reflects the gradually deepening understanding of the complex charge transport mechanisms in amorphous molecular semiconductors and provides a more refined theoretical basis for constructing more efficient photonic devices.

In amorphous materials or organic semiconductors, the Gaussian Disorder Model (EGDM) and the Correlated Disorder Model (ECDM) are used to describe charge transport characteristics, especially when the material's disorder is high and the interaction between carriers is weak. These models can predict the charge mobility or conduction behavior within a temperature range that is crucial for the performance of electronic devices. When the values of $p$ and $F$ tend towards zero, both EGDM

and ECDM can describe a temperature-dependent property. This property can be expressed through the proportional relationship $\mu \propto e^{-c\hat{\sigma}^2}$, where $\hat{\sigma} \equiv \sigma k_B / T$. In practical applications, this proportional relationship is valid within the interval $2 \le \hat{\sigma} \le 6$. Upon analyzing the two models (EGDM and ECDM), it was found that they are essentially the same in their $p$-dependence, and both show a non-Arrhenius form of temperature dependence, exhibiting a $(1/T^2)$ relationship [11,12]. Additionally, mobility is not solely influenced by temperature. At higher temperatures, thermal activation dominates charge transport. At lower temperatures, the effects of electric field strength and charge density become more pronounced, potentially leading to non-Arrhenius behavior [11-13]. Therefore, when analyzing charge transport in organic semiconductors, it is essential to consider parameters such as temperature, electric field strength, and charge density simultaneously to gain a more accurate understanding.

In the EGDM model, the mobility function $\mu(T, p, F)$ is based on simulation results of charge transport processes on a cubic lattice and applies the Miller-Abrahams transition rate [14]. Although this formula is widely used in drift-diffusion simulation software due to its ease of use, its assumptions of a regular cubic lattice and fixed localization radius may not accurately reflect its field dependence, which has also attracted some criticism in the academic community [15-17]. Furthermore, the lack of a variable range hopping (VRH) mechanism means that the model is somewhat inadequate in dealing with non-Gaussian density of states distributions, which constitutes a limiting factor in its application. Nenashev et al. [16] demonstrated within the GDM framework that the field-dependent mobility in a disordered system is related to the localization length $\alpha$, not the distance $b$ between sites. Ignoring $\alpha$ may lead to inaccuracies in mobility calculations, incorrect estimates of field dependence, insufficient representation of disorder effects, and limited applicability of the model, affecting material design and the consistency between theory and experiment. Therefore, to accurately describe charge transport characteristics, the parameter $\alpha$ should be included in the model. Referring to the concept of effective temperature by Shklovskii et al. [18,19], the influence of electric field and temperature on hopping mobility at finite temperatures can be represented by an effective temperature $T_{eff}(T, F)$, which includes the localization length $\alpha$ as a relevant spatial parameter. Therefore, to address the aforementioned issues and more precisely describe charge transport characteristics under high electric field conditions, we plan to develop a new simplified model. This new model will introduce the concept of effective temperature, which can thereby incorporate the localization length $\alpha$ into the model. The model will comprehensively consider the effects of electric field and temperature on transition mobility, with the localization length as a core parameter, to better align with experimental results and physical phenomena.

The study of amorphous molecular semiconductors is crucial for the development of organic light-emitting diode (OLED) technology. Tris(4-carbazoyl-9-ylphenyl)amine (TCTA), due to its excellent hole transport capability and photophysical properties, has been extensively studied in the field of OLEDs and used as a host material [7]. However, the poor solubility of TCTA poses challenges for its processing. Mile Gao and colleagues [20] successfully addressed this issue by synthesizing dendritic macromolecules with propyl groups while maintaining the photophysical characteristics of TCTA. Additionally, even when hole mobility reduction and phase separation phenomena occur in practical applications, the clever design of materials still enables the fabricated OLEDs to achieve an external quantum efficiency beyond expectations. Caterina Soldano et al. [21], in their research, significantly enhanced the light output in a transistor structure by adjusting the dye concentration in the green mixture (TCTA:Ir(ppy)3), indicating that it is feasible to improve the optoelectronic performance of organic light-emitting transistors through optimizing the emission layer design, paving new ways for applications in display technology and flexible electronic products. Guo He et al. significantly improved the quality of the PbI2-PbCl2 layer in perovskite photodetectors by adding TCTA nucleating agents and moisture, thereby greatly reducing the dark current density and achieving a large linear dynamic range, while maintaining long-term stability and fast response speed [22]. Given the low correlation caused by the disappearance of the TCTA molecular dipole moment, the analysis will adopt the simplest approximation of EGDM, i.e., ignoring the spatial and energy distribution correlations of electrons within the material [23]. Based on the results of ab initio microscopic simulations of hopping rates, an effective temperature model was developed to describe electrical properties. In the model, the concept of effective temperature is introduced to comprehensively reflect how temperature and electric field affect hopping rates. By adjusting the effective temperature, charge transport characteristics under different environmental conditions are simulated to more accurately predict the electrical behavior of TCTA amorphous small molecule layers. By changing the thickness, it is demonstrated that only assuming mobility depends on the electric field can fit the $J(V)$ characteristics of different thicknesses. These research findings showcase the potential of TCTA in optimizing OLED performance and pave new directions for the design and development of efficient OLED materials.

The structure of this paper is as follows: In Section 2, the improved mobility model is discussed and its application in hole transport in TCTA is demonstrated. The results of the temperature $T$, carrier concentration $p$, and field strength $F$ dependence of TCTA hole mobility $\mu$ obtained by solving the master equation for

site occupancy in large systems are provided. Parametric representations for these dependencies are also provided for convenient use in device simulations. In Section 3, the mobility function $\mu(T,p,F)$ is applied to describe the temperature and thickness dependence of the $J(V)$ characteristics of TCTA and the electrical performance of TCTA hole devices. Section 4 summarizes the main findings of this paper and concludes.

## 2. Improved expression of charge-carrier mobility

Charge transport in organic semiconductors occurs through an incoherent hopping mechanism, involving hops between two weakly coupled molecular sites $i$ and $j$. The hopping rate is denoted as $W_{ij}$ and can be described by Marcus theory, which considers the energy configuration of the system and the jump rate based on local state energies. The formula for the Marcus hopping rate is as follows [23,24]:

$$W_{ij} = \frac{2\pi}{\hbar}\frac{J_{ij}^2}{\sqrt{4\pi E_r k_B T}}\exp\left[-\frac{(\Delta E_{ij}-E_r)^2}{4E_r k_B T}\right] \quad (1)$$

The parameter $E_r$ represents the molecular reorganization energy, $\Delta E_{ij} = E_i - E_j$ defines the energy difference between sites $i$ and $j$, and $J_{ij}$ represents the charge transfer integral between these two sites. The energy difference $\Delta E_{ij}$ also includes a component influenced by an electric field $F$ applied in the $x$ direction, namely $-eFR_{ij,x}$, where $R_{ij,x}$ represents the distance between sites along the $x$ direction and $e$ denotes the magnitude of the elementary charge. Thus, the electric field $F$ affects the hopping rate $W_{ij}$ by influencing the energy difference $\Delta E_{ij}$, which ultimately affects the carrier mobility $\mu$. The electric field changes the energy difference between sites, thereby altering the likelihood of electron jumps between different sites.

The mobility function $\mu$ is obtained by solving the steady-state master equation that describes the site occupancy probabilities of charges in the simulation box. The master equation takes into account the strong Coulomb repulsion on the sites, thus not allowing two charges to occupy the same site simultaneously. We randomly select site energies from a Gaussian distribution with a standard deviation of $\sigma$. The method described in reference [11] is used to randomly generate site positions and direct transfer integrals. The master equation (ME) describes how the charge occupancy probabilities of various sites in the simulated charge transport system are interdependent through charge hopping processes and reach equilibrium under steady-state conditions. By solving this equation, we can obtain the mobility function $\mu$ of the system, which further describes the movement of charge carriers within the material under external conditions such as electric fields. Under steady-state conditions, the master equation (ME) can be represented as:

$$\sum_{j\neq i}[W_{ij}p_i(1-p_j) - W_{ji}p_j(1-p_i)] = 0 \quad (2)$$

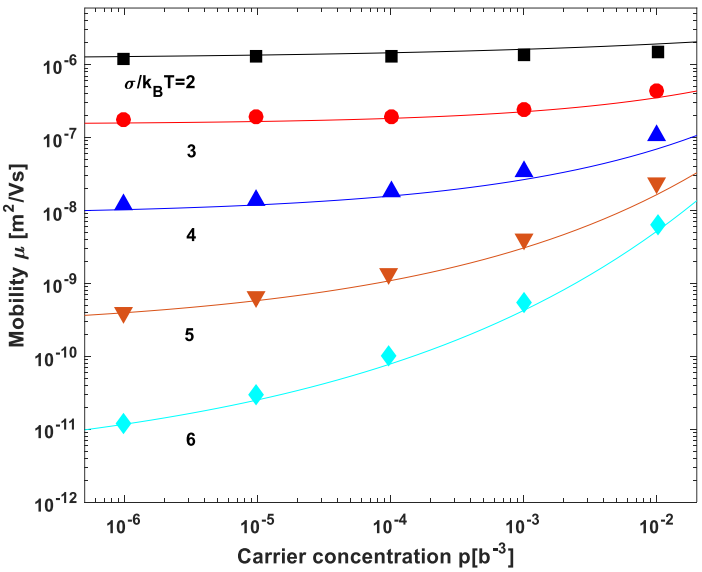


*Fig. 1. Shows the relationship between hole mobility $\mu$ and carrier concentration $p$ at different temperatures $T$ for TCTA material under zero electric field ( $F=0$ ) conditions. The data points are obtained by simulating electron transfer in random material structures and averaging the results[25]. The curves are fitted using the parameterized equation (5a), where $\mu^* = 6.1\times10^{-6}\,m^2/Vs$, $c=0.41$ (colour online)*

where $p_i$ represents the probability of site $i$ being occupied by a charge, and $W_{ij}$ is the hopping rate from site $i$ to site $j$. The factor $(1-p_i)$ takes into account Coulomb repulsion, ensuring that each site can be occupied by at most one charge. $W_{ij}p_i(1-p_j)$ and $W_{ji}p_j(1-p_i)$ calculate the expected number of hops from site $i$ to $j$ and from site $j$ to $i$, respectively. The equilibrium condition $[W_{ij}p_i(1-p_j)-W_{ji}p_j(1-p_i)]=0$ indicates that the net hopping rate between all pairs of sites is zero, meaning the system has reached dynamic equilibrium.

In Fig. 1, the effects of different temperatures $T$ and carrier concentrations $p$ on the result $\mu$ were studied. The symbols represent the ME results of $\mu$ as a function of $p$ at different $\hat{\sigma}=\sigma/k_BT$ values for TCTA when the electric field $F=0$. The curves represent the results fitted using the parameterization scheme given in reference [11]:

$$\mu(T,p,F)\approx\mu(T,p)f(T,F) \tag{3}$$

$$\mu_0(T)=\mu^*\exp(-c\hat{\sigma}^2) \tag{4}$$

$$\mu(T,p)=\mu_0(T)\left[\frac{1}{2}(\hat{\sigma}^2-\hat{\sigma})(2pb^3)^{\delta}\right] \tag{5a}$$

$$\delta=2\hat{\sigma}^{-2}[\ln(\hat{\sigma}^2-\hat{\sigma})-\ln(\ln 4)] \tag{5b}$$

with $\mu^*=6.1\times10^{-6}m^2/Vs$, $c=0.41$, the revised value of $c$ is very close to the value $c=0.42$ used in previous simulations by Pasveer et al. [11], therefore the dependence on $T$ is very similar to EGDM. However, although the model of Pasveer et al. can describe charge transport well at low densities, its fit in the high-density region is less satisfactory. This is because their model only considers the non-Arrhenius temperature dependence $\ln(\mu)\propto 1/T^2$ (see Equation (4)), which may not be applicable at high densities. Therefore, for the high-density region, further modifications to the model or the introduction of additional mechanisms may be needed to more accurately describe the charge transport behavior.

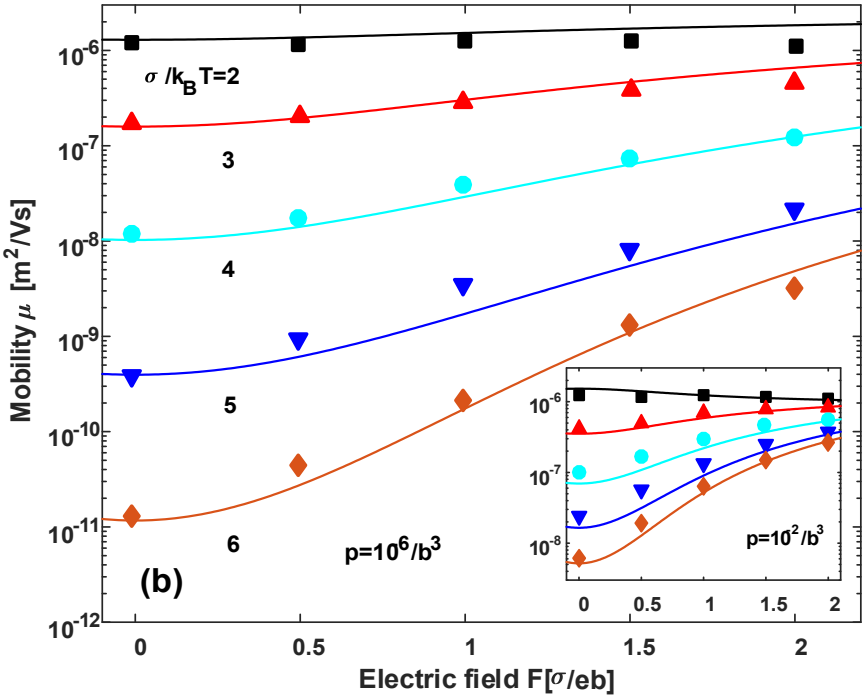


*Fig. 2. Depicts how the mobility $\mu$ in TCTA is affected by different temperatures $T$ at low and high carrier concentrations $p$ as the electric field $F$ changes. The points in the figure represent the results of the master equation [25]. The curves on the left (a) use Equations (3)-(6) from reference [11] with parameters $A=0.35$ and $B=1.4$. The curves on the right (b) are based on a modified set of equations (colour online)*

In Fig. 2, the influence of the dimensionless electric field $F$ on the mobility $\mu$ is shown for low (main plot) and high (inset) carrier concentrations $p$ at various temperatures. Here, $b\equiv N_t^{-1/3}$, with parameters $A=0.35, B=1.4$ on the left (a). It is noted that, similar to EGDM [11], a prefactor $f(T,F)$ independent of density was utilized to describe the electric field dependence. The compact parameterization deviates from ME results within a large range of $F$ values but is sufficiently precise within the scope of experimentally relevant electric fields up to $Feb/\sigma\approx1$. It is evident that Equation (5) becomes invalid when $Feb>\sigma$ and $\sigma>1.7/k_BT$, turning the exponential positive, which results in the equation predicting an exponential increase

in mobility as the electric field strengthens, leading to incorrect infinite limits for any electric field. In the region of low electric fields, where $\ln\mu$ is proportional to $ABF^2$, the factor $AB$ signifies the sensitivity to the electric field. For EGDM, the parameterization used values $A=0.44$ and $B=0.8$ [11]. This factor is 0.49, compared to 0.35 for EGDM. Thus, it can be concluded that the mobility of TCTA exhibits a greater dependency on $F$.

$$f(T,F)=\exp\left\{A(\hat{\sigma}^{3/2}-2.2)[\sqrt{1+B(ebF/\sigma)^2}-1]\right\} \quad (6)$$

In organic semiconductors, charge transport typically occurs through a hopping mechanism, where the transition of charges between different localized states plays a crucial role. This hopping process is not only influenced by the electric field but also related to the transmission distance of charges within the material. Therefore, the spatial scale parameter $\alpha$ is particularly important here, as it reflects the extent of the electric field's impact on the hopping mobility. Mobility, as a measure of the average drift velocity of carriers under the action of an electric field, is closely related to the spatial scale associated with the electric field.

To better describe the dependence of carrier mobility on the electric field $F$, the concept of effective temperature $T_{eff}(T,F)$ was introduced. Effective temperature is a theoretical tool used to describe the temperature experienced by carriers under the influence of an electric field, which may differ from the physical temperature of the material. This parameter takes into account the impact of the electric field and the spatial scale parameter $\alpha$ on the energy state of the carriers, thereby more accurately reflecting the motion state of carriers in the electric field.

Despite localized length $\alpha$ being a key parameter affecting hopping mobility, it does not appear in Equation (6), leading to discrepancies between simulations and actual scenarios. To address this, we proposed a weak density-dependent function, Equation (7), which not only replaces Equation (6) but also introduces electric field dependence. This improvement allows for more accurate simulation of carrier migration behavior, especially under high electric field conditions.

In this way, Equations (7)-(10) provide an improved description of electric field dependence, as shown in Fig. 2(b), outperforming Equations (3)-(6) in describing electric field dependence. This enhancement not only strengthens the model's predictive power but also provides a more solid theoretical foundation for the design and optimization of organic electronic devices. In summary, by introducing effective temperature and considering electric field dependence, it is possible to simulate and predict carrier migration behavior in organic semiconductors more accurately, especially under high electric field conditions. This methodological improvement is significant for understanding and designing organic electronic devices, offering new perspectives and tools for future development and application.

$$g(T_{eff},F)=\left[1+c_1\left(\frac{ebF}{\sigma}\right)^2\right]^{-1/2} \quad (7)$$

$$\mu(T_{eff},p,F)=\mu(T_{eff},p)^{g(T_{eff},F)}\exp\left[c_2 g(T_{eff},F)-1\right] \quad (8)$$

where $c_1$ and $c_2$ are weakly density-dependent parameters that explicitly depend on the dimensionless quantities $\hat{\sigma}'\equiv\sigma/k_BT_{eff}$ and the carrier concentration $pb^3$.

$$c_1=1.26+0.732\hat{\sigma}'-0.257\hat{\sigma}'^2+0.025\hat{\sigma}'^3+0.09\ln(pb^3), \quad (9)$$

$$c_2=14.26+0.262\hat{\sigma}'-0.179\hat{\sigma}'^2+0.017\hat{\sigma}'^3+0.09\ln(pb^3), \quad (10)$$

## 3. Analysis of experimental SCLC data

In single-carrier devices with ohmic contacts, the current is primarily limited by the internal transport within the semiconductor, a phenomenon commonly referred to as space-charge-limited current (SCLC). In such devices, the current density ($J$) follows the Mott-Gurney square law [26]:

$$J=\frac{9}{8}\varepsilon\mu\left(\frac{V^2}{L^3}\right) \quad (11)$$

where $\varepsilon$ represents the dielectric constant of the material, $V$ represents the applied voltage, and represents the thickness of the layer. In this formula, the current density is directly proportional to the square of the applied voltage and inversely proportional to the cube of the layer thickness. In this study, hole-only devices consist of a single layer of hole transport material sandwiched between an ITO/PEDOT:PSS bottom electrode and an enhanced MoO3/Al top electrode. For hole-only devices using TCTA as the intermediate layer, this configuration allows for the direct application of fundamental equations from semiconductor physics and electronic engineering to describe charge transport and electric field distribution within. Specifically, these equations involve the current density, the rate of change of electric field strength, and the calculation of voltage, providing a solid theoretical foundation for a deep understanding of TCTA's hole transport characteristics and its applications in electronic devices. This, in turn, supports the design of efficient and stable organic electronic technologies.

$$J = p(x)e\mu(T_{eff}, p(x), F(x))F(x) \tag{12a}$$

$$\frac{dF}{dx} = \frac{e}{\varepsilon_0 \varepsilon_r} p(x) \tag{12b}$$

$$V = \int_0^L F(x)dx \tag{12c}$$

Here, $x$ represents the distance from the injection electrode, and $p(x)$ refers to the hole concentration at position $x$ in the organic film layer; is the vacuum permeability, and is the typical relative dielectric constant value for organic semiconductors, while represents the thickness of the polymer layer between two electrodes. Diffusion effects significantly increase the current only at low voltages, and near the electrodes, variations in density and electric field are negligible [11].

In subsequent research, the enhanced mobility model presented in Section 3 will be employed to thoroughly examine hole transport in TCTA materials. This refined model will be integrated with coupled equations that describe space charge limited current (SCLC), and experimental $J(V)$ measurements for single-device TCTA-based holes under various temperatures will be illustrated in Fig. 3. It is specifically noted that the data in the figure are plotted on a logarithmic scale to better elucidate the scope and trends of the measurements.

It is important to use the same set of parameters for simulations at each temperature, ensuring consistency when comparing data under different conditions. For small molecule materials, the Density of States (DOS) width typically ranges between 0.08-0.15eV. Therefore, the value of $\sigma$ (0.11eV) adopted in the improved model is physically reasonable and aligns with the known characteristics of small molecule materials.

To further validate the accuracy of the model parameters, this set of parameters was also utilized to describe the current-voltage characteristics of layers with varying thicknesses. The symbols in Fig. 4 display the $J(V)$ characteristics measured at room temperature for devices featuring different TCTA layer thicknesses (102-303nm). Adjusting the molecular layer thickness revealed that assuming mobility μ depends on the electric field $F$ accurately fits the $J(V)$ characteristic curves for hole-only devices of differing thicknesses without requiring any changes to the fitting parameters. This rigorous approach ensures the model's effectiveness and accuracy in describing hole transport in TCTA, laying a robust foundation for additional research and applications.

*Table 1. Comparison of parameters energetic disorder (σ), effective lattice contact (b), pre-factor mobility ($\mu^*$), room temperature hole mobility (μ)*

| Results | | $\sigma$[eV] | $\mu^*$ [$10^{-6}m^2V^{-1}s^{-1}$] | $\mu(295K)$ [$10^{-8}m^2V^{-1}s^{-1}$] | $b$[nm] |
|---|---|---|---|---|---|
| N.B.Kotadiya et al. [25] | exp | 0.1 | 5.94 | 0.893 | 1.4 |
| | sim | 0.112 | – | 1.01 | 1.34 |
| A.Masse et.al.[23] | sim | 0.136 | 6.1 | – | – |
| This work | sim | 0.11 | 6.1 | 0.844 | 1.4 |

In Table 1, we meticulously compared the key parameters employed in three different studies (Kotadiya et al. [27], Masse et al. [25], and our current work): $\sigma$ (energy disorder parameter), $b$ (lattice constant), and $\mu^*$ (mobility prefactor). In investigating the hole transport characteristics in TCTA materials, we observed significant consistency between our experimental data and the improved model we proposed. This consistency is particularly evident in the $\sigma$ parameter, with a value close to 0.112eV used by Kotadiya et al. [27] and significantly lower than the 0.136eV used by Masse et al. [25]. This finding reveals the precision of our model in describing a DOS width of 0.1eV, which aligns closely with analyses predicted based on the EGDM (Effective Gate Dielectric Method).

Furthermore, this similarity in energetic disorder is also reflected in the mobility observed at room temperature. The mobility observed is within the range of approximately $0.893\times10^{-8}\,m^2V^{-1}s^{-1}$, which is consistent with previous research results, indicating that the improved model can accurately capture the charge transport characteristics of the material. Additionally, it was noticed that the inter-site distance remains at about 1.4 nm, both in the microscopic model and in the EGDM model. This distance corresponds to the average distance over which charges hop under the influence of an electric field, providing strong evidence for understanding the charge transport mechanism.

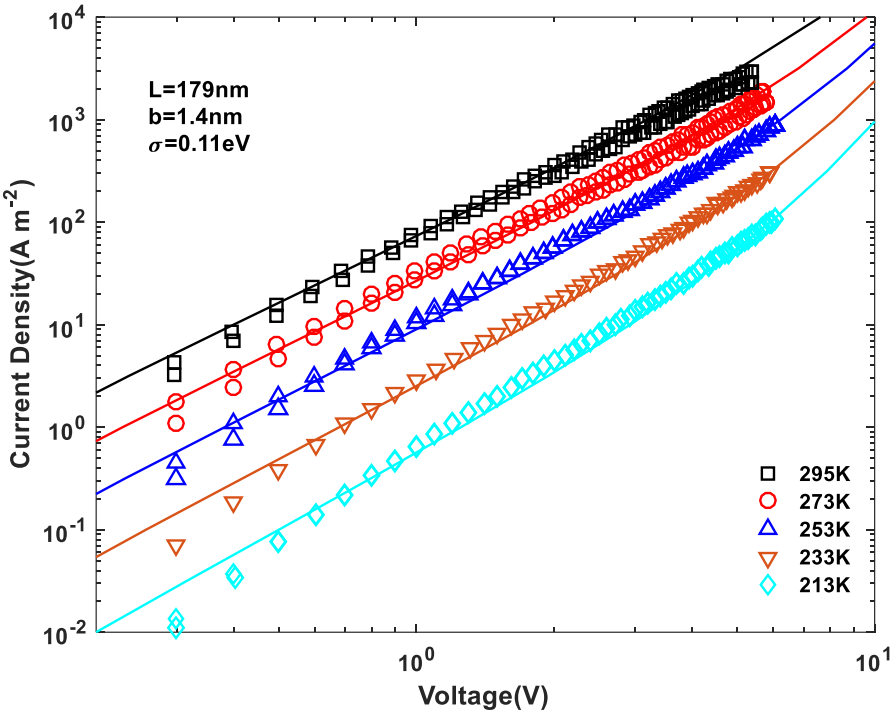


*Fig. 3. Displays a comparison between experimental data (symbols) and theoretical predictions (lines) for the Space-Charge-Limited (SCL) current as a function of voltage in TCTA (Tris(4-carbazoyl-9-ylphenyl)amine) material. The symbols represent the experimental results from reference [27], while the lines depict the solution to the SCLC equation (Equation (12)) that considers the temperature ( $T$ ), carrier concentration ( $p$ ), and electric field ( $F$ ) dependence of mobility $\mu$ in the present work. The mobility parameter used in these calculations, denoted as $\mu^*$, has a value of $6.1\times10^{-6}\ m^2/Vs$ (colour online)*

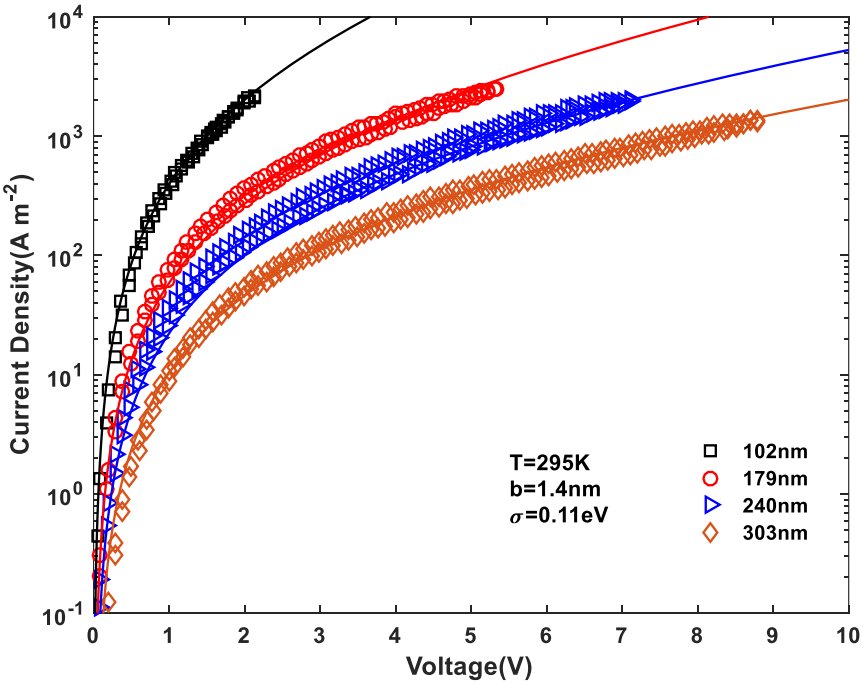


*Fig. 4. Illustrates the current density-voltage character- istics of TCTA at various thicknesses at room temperature, represented by symbols from reference [27]. The figure also includes the results of the improved EGDM simulations, shown in the form of lines. These simulations demonstrate excellent agreement with the experimental data across a range of different film thicknesses, utilizing the same set of parameters cited in the main text (colour online)*

Finally, these results emphasize the importance of a more precise representation of mobility. By improving the expression of mobility, better simulation and prediction of charge transport behavior in organic semiconductor materials can be achieved, which is significant for optimizing device performance and designing efficient electronic devices. In summary, this work not only demonstrates the good consistency between the improved model and experimental data but also highlights the importance of accurate model parameters for understanding and predicting the behavior of organic electronic materials.

Figs. 5 and 6 demonstrate how the $J(V)$ characteristics of hole-only devices based on TCTA change with the interfacial carrier density $p_0$ at different layer thicknesses and temperatures. From these figures, it can be observed that the voltage shows an increasing trend with the current, and its variation is related to $p_0$. When $p_0$ reaches a moderate level, there is generally little association between voltage and $p_0$, leading to a flat $V-p_0$ curve. The $J(V)$ relationship enters the expected Ohmic region when the balance between injected carriers near the device surface and discharge is achieved. Notably, to maintain the same $p_0$ and constant current density $J$ under low and high temperature conditions, a stronger electric field enhancement and correspondingly higher voltage are required at lower temperatures than at higher temperatures, indicating a higher effective mobility at elevated temperatures. Similarly, thicker devices require a stronger electric field, whereas thinner devices do not; additionally, the effective mobility in thicker devices is also lower than in thinner ones. Since the mobility in disordered organic materials is influenced by density, very thick devices have a lower average hole density. In some cases, the impact of mobility, carrier density, and electric field enhancement effects can be disregarded. As the device thickness decreases, the actually measured current density significantly exceeds the expected value.

In Figs. 7 and 8, a detailed analysis is conducted on the influence of position (distance from the interface) within TCTA-based hole-only devices on carrier density and electric field. Special attention must be paid to the mobility in the device's central region, where $p_0$ is approximately $1\times10^{23}$-$1\times10^{24}\mathrm{m}^{-3}$, to ensure that the $J(V)$ characteristics are physically realistic. Consequently, two different values of $p_0$, namely $(0.5,10)\times10^{23}\mathrm{m}^{-3}$, were used in the calculations. In the case of disordered materials, there are no explicit equations relating carrier density $p(x)$ and electric field $F(x)$ numerical results indicate that $p(x)$ gradually decreases with increasing distance $x$, while the distribution of $F(x)$ increases with distance $x$ from the ITO injecting anode.

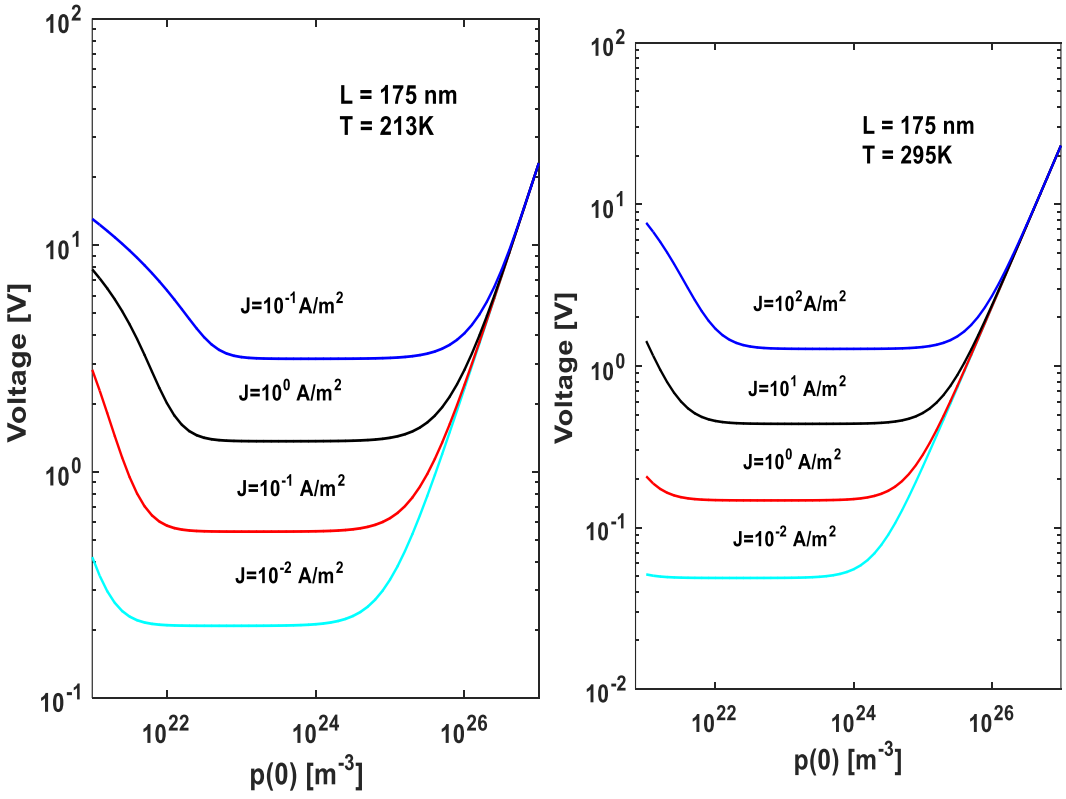


*Fig. 5. Demonstrates the theoretical research results of voltage variation with charge density at the position of $x=0$ for 175nm thick TCTA material under the conditions of 213K and 295K. The curves of different colors in the figure represent different current density $J$ values, with the unit of $\mathrm{A/m}^3$ (colour online)*

For larger values of $p_0$, the rate of change is greater; for smaller values of $p_0$, the rate of change is less. Poisson's equation (Equation (11b)) suggests that the electric field monotonically increases with changing position and links the electric field to carrier density. Thus, carrier injection from the electrode to the TCTA layer leads to enhanced space charge near the interface, causing a decreasing trend in $p(x)$. The distribution of $p(x)$ and the enhancement of space charge near the interface contribute to the variation in $F(x)$. These findings are similar to the phenomena of carrier density and field-dependent mobility described by Tanase et al. [28] in drift systems.

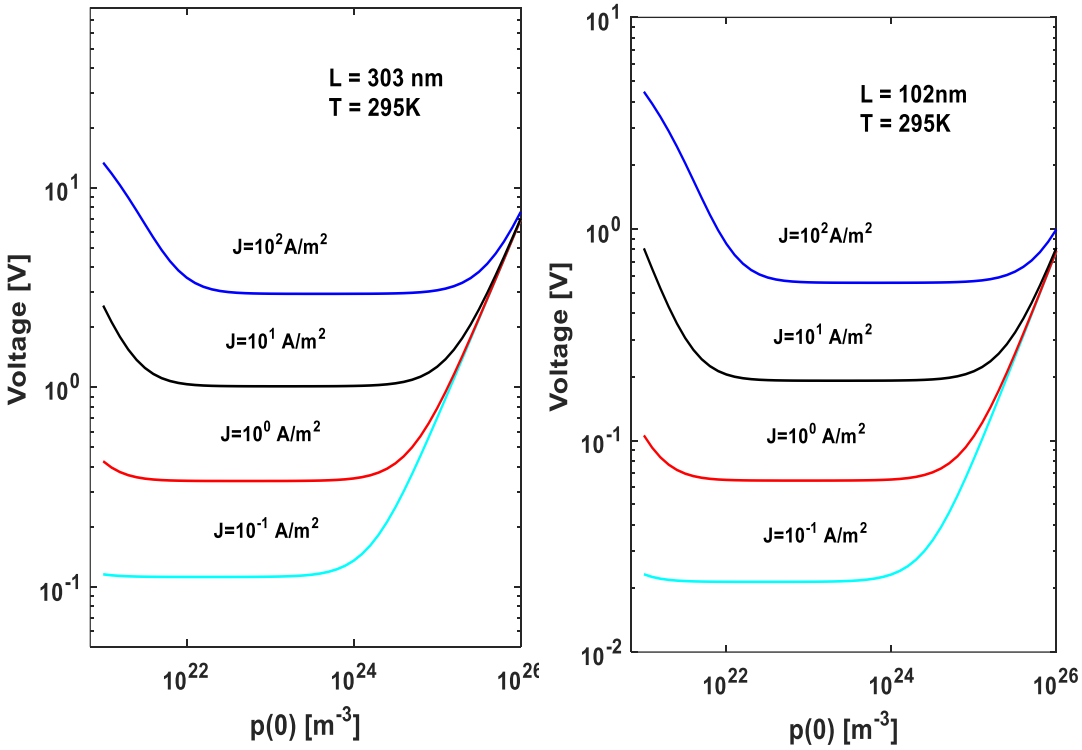


*Fig. 6. Displays the theoretical analysis results of voltage variation with charge density for TCTA layers of 303nm and 102nm thickness at room temperature. The curves of different colors in the figure represent different current density $J$ values, with the unit of $\mathrm{A/m^3}$ (colour online)*

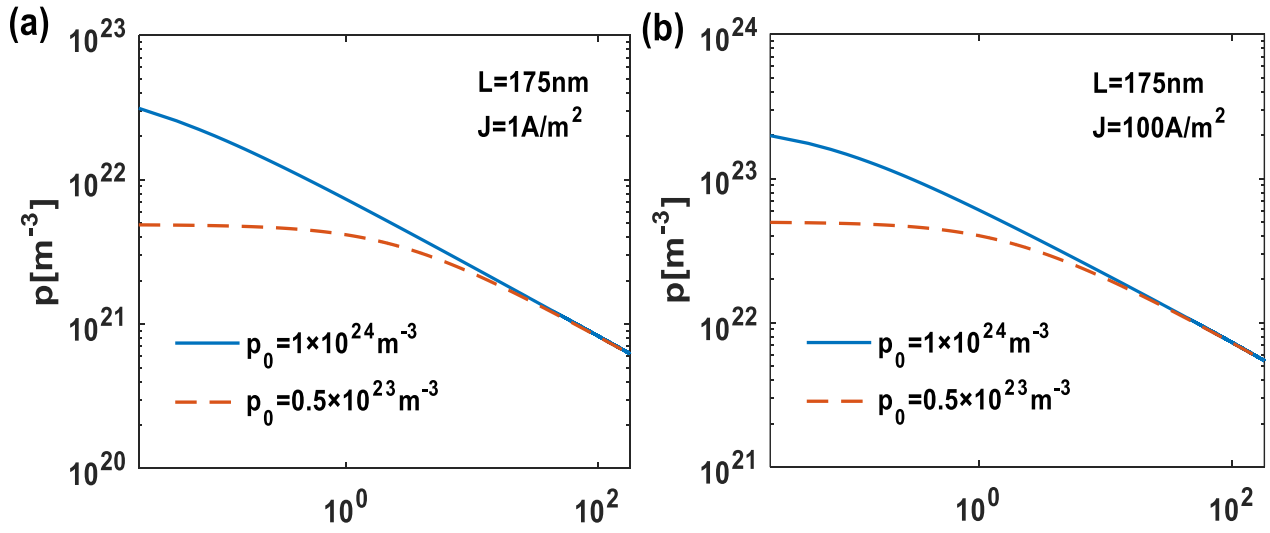

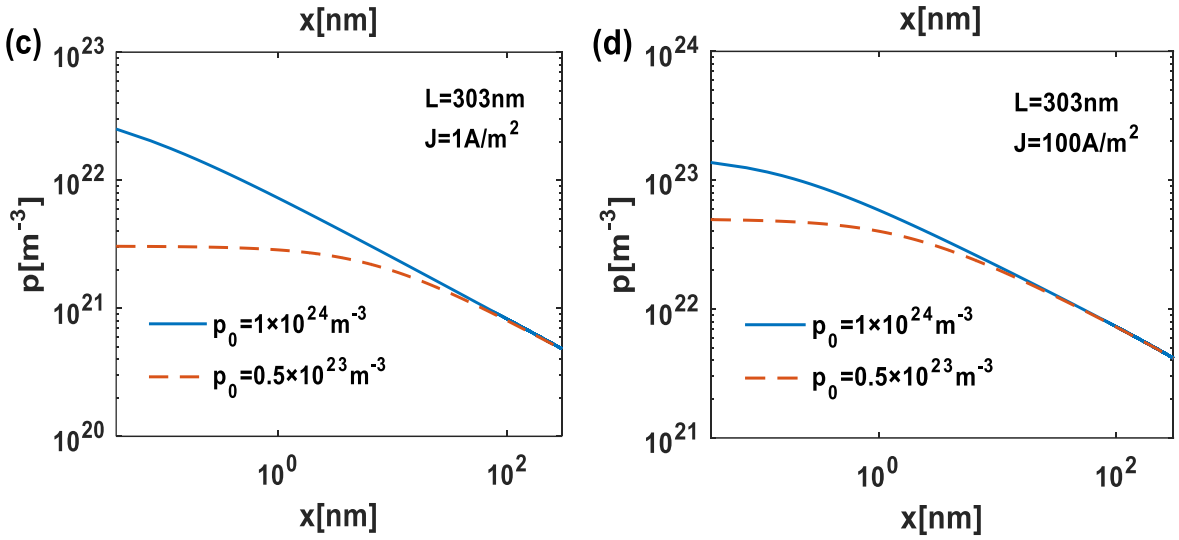


*Fig. 7. Illustrates the distribution of carrier density $p$ along position $x$ in hole-only devices based on TCTA material at room temperature for different device thicknesses under low and high current densities. The solid lines in the figure represent a boundary carrier density of $p_0 = 1\times10^{24}\,m^3$, while the dotted lines correspond to $p_0 = 0.5\times10^{23}\,m^3$ (colour online)*

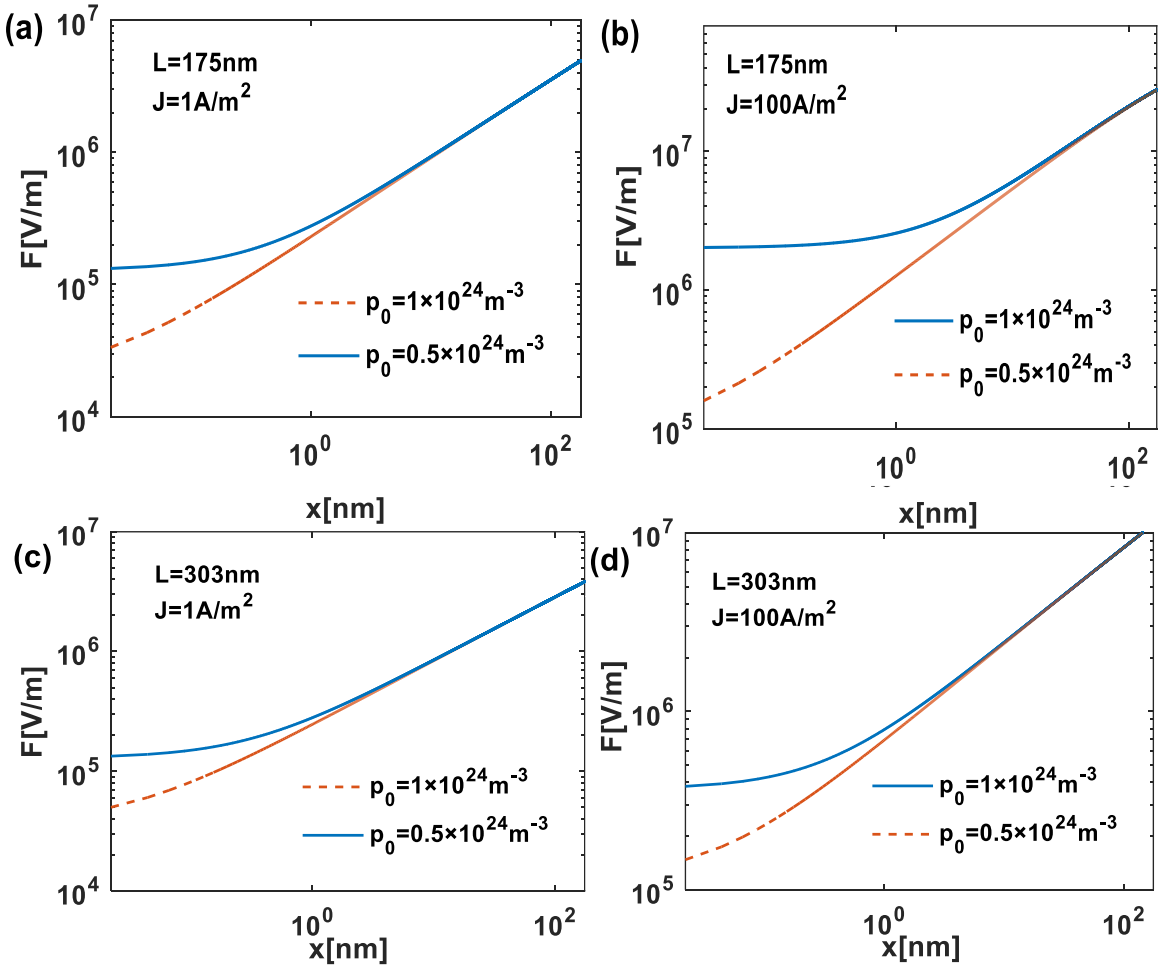


*Fig. 8. Demonstrates the calculated distribution of electric field $F$ as a function of position $x$ in hole-only devices based on TCTA at room temperature, taking into account different thicknesses and low to high current densities. The solid lines represent scenarios with a boundary carrier density of $p_0 = 0.5\times10^{23}\,m^3$, while the dashed lines indicate situations where $p_0 = 1\times10^{24}\,m^3$ (colour online)*

## 4. Summary and conclusions

Through computer simulation and analytical calculation, we have reached a conclusion: even in the presence of uncorrelated energetic disorder, it is feasible to improve the modeling of hole-only $J-V$ characteristics for TCTA devices. We heuristically obtained an algebraic mobility prefactor by numerically solving the master equation and fitting within a relevant parameter range. Research has shown that the original effective Gaussian disorder model (EGDM) can well describe the dependence of mobility on temperature ( $T$ ) and carrier density ( $p$ ), while also significantly simplifying the lattice structure of the model. However, for the material systems discussed in this paper, EGDM exhibits relatively weak electric field ( $F$ ) dependence. Therefore, it is necessary to replace the original temperature variable with an effective temperature that includes the effects of the electric field to enhance the sensitivity of carrier mobility $\mu$ to the electric field. This point is confirmed by obtaining lower Gaussian state density values in other organic semiconductor materials. We also conducted multiscale simulations, simulating the trends of carrier density and electric field changes with distance, which achieved a high degree of consistency with experimental measurements. Constructing an accurate mobility theoretical model is crucial for predicting charge transport and device characteristics, and it can also be used to verify errors caused by improper experimental operations. Based on these findings, we hope that our theory can help design and synthesize better materials and further improve device performance.

**Acknowledgements**

This work is supported by Project No. PX-1292025012, “AI-Enhanced Integrated Science-Industry-Education Practical Teaching Base for the Automation Specialty Cluster, collaboratively established by Guangdong Ocean University and Shenzhen Yonghang New Energy Technology Co., Ltd.”.

## References

[1] S. Jung, Y. Lee, A. Plews, A. Nejim, Y. Bonnassieux, G. Horowitz, IEEE Transactions on Electron Devices **68**, 307 (2021).

[2] T. J. Fan, Q. Cheng, D. Lian, Y. W. Z, National Science Review **8**, 2095 (2025).

[3] Y. J. Hu, Z. X. Chen, Y. Xiang, C. H. Cheng, W. F. Liu, W. S. Zhan, Journal of Semiconductors **44**, 082701 (2023).

[4] Y. Bae, S. A. Park, S. Kim, H. Lim, J. Kim, L. Ye, T. Park, Advanced Energy Materials **15**, 2405217 (2025).

[5] Y. Hua, H. Kim, Z. Ruan, B. Kang, G. B. Zhang, Y. Ding, ACS Applied Materials and Interfaces **17**, 31183 (2025).

[6] S. H. Kang, S. M. Lee, K. C. Lee, C. D. Yang, ACS Applied Materials and Interfaces **17**, 44030 (2025)

[7] J. Saghaei, M. Koodalingam, P. L. Burn, A. Pivrikas, P. E. Shaw, Organic Electronics **100**, 106389 (2022).

[8] H. Bässler, Physica Status Solidi B **175**, 15 (1993).

[9] Y. N. Gartstein, E. M. Conwell, Chemical Physics Letters **245**, 351 (1995).

[10] S. Novikov, D. Dunlap, V. Kenkre, P. E. Parris, A. V. Vannikov, Physical Review Letters **81**, 4472 (1998).

[11] W. F. Pasveer, J. Cottaar, C. Tanase, R. Coehoorn, P. A. Bobbert, P. W. M. Blom, D. M. de Leeuw, M. A. J. Michels, Physical Review Letters **94**, 206601 (2005).

[12] M. Bouhassoune, S. L. M. van Mensfoort, P. A. Bobbert, R. Coehoorn, Organic Electronics **10**(3), 437 (2009).

[13] J. Cottaar, R. Coehoorn, P. A. Bobbert, Physical Review B **85**, 245205 (2012).

[14] A. H. Miller, Physical Review **120**, 745 (1960).

[15] A. V. Nenashev, F. Jansson, J. O. Oelerich, D. Huemmer, A. V. Dvurechenskii, F. Gebhard, S. D. Baranovskii, Physical Review B **87**, 235204 (2013).

[16] A. V. Nenashev, J. O. Oelerich, A. V. Dvurechenskii, F. Gebhard, S. D. Baranovskii, Physical Review B **96**, 035204 (2017).

[17] S. D. Baranovskii, Physica Status Solidi A **215**, 1700676 (2018).

[18] S. Marianer, B. I. Shklovskii, Physical Review B **46**, 13100 (1992).

[19] S. D. Baranovskii, B. Cleve, R. Hess, P. Thomas, Journal of Non-Crystalline Solids **164**, 437 (1993).

[20] M. Gao, J. Jang, T. Leitner, V. T. N. Mai, C. S. K. Ranasinghe, R. Chu, P. L. Burn, A. Pivrikas, P. E. Shaw, Advanced Materials

Interfaces **8**, 2100820 (2021).
[21] C. Soldano, O. Laouadi, K. Gallegos-Rosas, ACS Omega **7**, 43719 (2022).
[22] G. He, L. Han, C. Lin, K. Tao, Nanoscale **26**, 5786 (2024).
[23] A. Masse, P. Friederich, F. Symalla, F. Liu, V. Meded, R. Coehoorn, W. Wenzel, P. A. Bobbert, Phys. Rev. B **95**, 115204 (2017).
[24] R. A. Marcus, J. Electroanal. Chem. **65**, 13 (1993).
[25] A. Massé, P. Friederich, F. Symalla, F. Liu, R. Nitsche, R. Coehoorn, W. Wenzel, P. A. Bobbert, Physical Review B **93**, 195209 (2016).
[26] N. F Mott, R. W. Gurney, Journal of Chemical Education **18**, 1941(1948).
[27] N. B. Kotadiya, M. Anirban, S. Xiong, P. W. M. Blom, D. Andrienko, G.-J. A. H. Wetzelaer, Advanced Electronic Materials **4**, 1800366 (2018).
[28] C. Tanase, P. W. M. Blom, D. M. D. Leeuw, Physical Review B **70**, 193202 (2004).

*Corresponding author: lhluo@gdou.edu